Electrocristallization of Copper from Non-Cyanide Alkaline Solution Containing Glycine

J.C. Ballesteros[1], E. Chainet[2], P. Ozil[2], Y. Meas[1,*] and G. Trejo[1,*]

[1] Centro de Investigación y Desarrollo Tecnológico en Electroquímica (CIDETEQ), Parque Tecnológico Sanfandila, Pedro Escobedo, Querétaro, C.P. 76703 Querétaro, México
[2] Laboratoire d'Electrochimie et de Physicochimie des Matériaux et des Interfaces, LEPMI, UMR 5631 CNRS-INPG-UJF, BP 75, 38402 Saint-Martin d'Heres Cedex, France
[*] E-mail: yunnymeas@cideteq.mx ; gtrejo@cideteq.mx

A thermodynamic study by means of potential-pH (Pourbaix type) and species repartition diagrams is presented in this work with the view to better understand the electrodeposition of copper from non-cyanide alkaline solution containing glycine. The parameters studied were glycine concentration, temperature and scanning rate. The voltametric studies also indicate control by diffusion for the copper electrodeposition. In order to compare the effect of the temperature, we measured the kinetic parameters: charge transfer coefficient (α_c) and rate constant ($\vec{k}$). The morphological study indicated that the temperature plays a role on grain size of the copper coating obtained. X-ray diffraction studies showed that the deposit obtained at 40°C has a crystallite structure, which differs from that found at 25°C.

1. INTRODUCTION

Electrodeposition of copper from alkaline cyanide solutions have been widely used for industrial level production of coatings of high quality. Cyanide copper plating is used throughout the metal finishing industry for many applications, although not as extensively today as in the 1970s because of environmental issues [1]. Site contamination, worker safety considerations, and high waste treatment and reporting costs are some drawbacks. Alkaline noncyanide copper-plating solutions have found increasing popularity since mid-1980s because of environmental issues [1]. Disadvantages include higher operating costs, difficulty in using the process on zinc die castings, greater sensitivity to impurities, and a chemistry more difficult to control [1]. In recent years a large amount of research has been realized around the world and different alternatives have been proposed, such as: fluoborate,

pyrophosphate, EDTA, citrate, ammonia, ethylenediamine, glycerol, tartrate, etc. [1]. However, the majority of these proposals have not been applied to industrial level.

The glycine (H_2G^+) has been used as a complexing agent in the electrodeposition of Zn-Ni [2], Cu-Co [3], Zn-Co alloys [4], and more recently by our research group to obtain Zn-Co alloy [5]. These studies show that the deposits obtained from alkaline bath containing glycine are of high quality.

Few articles [6-12] has been reported on the electrochemical reduction of Cu(II) from glycinate electrolytes. Survila-Uksiene [7] found, by means of an RDE technique, that the electrochemical reduction process at pH < 8.3 occurs from CuG^+ complex and proceed through two consecutive one-electron transfers. They observed that the reduction kinetics of CuG^+ depends of formation of Cu_2O onto the copper electrode surface. Kublanovsky-Litovchenko [9] proposed three ways of transforming of Cu(II)-glycine complexes in an alkaline medium, where CuG_2 and CuG_3^- predominate; they proposed that at low polarizing current densities and high alkali concentrations, the formation of Cu_2O is possible. The second way is the disproportionation process. The third way is the attachment of the second electron and which depends on the electrode potential. Drissi-Daoudi et al. [10] observed the electrochemical behavior of copper in solution containing Cu(II)-glycine at pH 10.0. They proposed that cuprous complex is an intermediate in the cupric complex reduction but is not detected during the oxidation of electrodeposited copper in this solution.

Despite these many important contributions to the study of electrochemical reduction of copper-glycine complexes, a detailed analysis on the quality of the coatings obtained during copper electrodeposition is still not done. We consider important the effect of the temperature because in the literature [1] is mentioned that one of the operating conditions of alkaline non-cyanide copper plating baths is temperature higher than 38ºC.

The aim of the present work is three-fold. In a first part, we present a thermochemical study on the copper-glycine-water system by means of species distribution and potential-pH diagrams with the view to better understand the effect of the different parameters on the deposition mechanism. In a second part, we present an electrochemical study in order to obtain kinetic parameters. Finally, in a third part, we present a morphological study of the copper coatings obtained. Nickel electrode was utilized because the copper coating at industrial level containing an undercoat layer of nickel.

2. EXPERIMENTAL

The electrochemical study of the reduction of Cu (II) ions in the presence of glycine was carried out in a conventional three-electrode cell from the solutions shown in Table 1. All solutions were prepared using analytic grade reagents (provided by Sigma-Aldrich Company) with ultra pure water (Millipore-Q system) and were deoxygenated by bubbling N_2 for 20 minutes before each experiment. The working electrode was a nickel disk provided by Sigma-Aldrich, made of a nickel rod embedded in Teflon. The exposed surface area (0.317 cm^2) was polished to mirror finish with different grades of alumina down to 0.05 μm and ultrasonically cleaned before experiments. A graphite bar with an exposed area greater than the working electrode was used as counter electrode. A saturated calomel electrode (SCE) was used as reference, and in this work all potentials are refer to this scale. The

electrochemical experiments were carried out with a potentiostat/galvanostat PAR273A (EG&G) connected to a personal computer running the general purpose electrochemical system software Power Suite for control of experiments and data acquisition. The conditions for electrochemical experiments are chosen in where the ohmic drop is considered negligible. Rotating disc electrode (RDE) voltammetry was performed using a Tacussel model EDI (C; 3 mm diameter) containing a thin Cu deposit on the disk. Copper coatings on nickel substrates were obtained and this was realized in order to evaluate the quality and morphology of these deposits. The solution temperature was controlled and made constant with a circulating water thermostat (Bioblock Scientific). A ZEISS ultra-55 scanning electron microscope (SEM) was used to determine the coating morphology, such as shape and size. The X-ray diffraction (XRD) experiments were carried out with a Bruker D8 Advance type diffractometer, using a Cu Kα radiation ($\lambda = 1.5418$Å). The diffraction pattern was scanned by steps of 0.02º (2θ) between 40 and 77º.

Table 1. Chemical composition of solutions used in this work

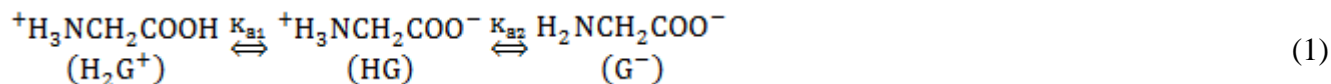| Solution	$[Cu^{2+}]$ mol L^{-1}	$[Cu^{2+}]$ mol L^{-1}	$[Cu^{2+}]$ mol L^{-1}	pH
S_0	-	-	1.2	10.0
S_1	0.1	0.2	1.2	10.0
S_2	0.1	0.2	2.2	10.0

The kinematic viscosity of the solution was measured on a capillary viscosimeter (Schott-Gerräte GmbH) baring a capillary tube (538.10, Schott) at 25 and 40°C. The viscosity measurement consists of the determination of the time for a solution to flow through the capillary tube. The uncertainty in the flow time measurement is estimated to be 0.01 s. This little value leads to a relative standard uncertainty of less than 0.01% in the viscosity measurement and can therefore be neglected. The experimental kinematic viscosity values obtained are the average of ten successive measurements of the flow time. The obtained values were 0.0113 ± 0.0002 and 0.0079 ± 0.0001 cm^2 s^{-1} at 25 and 40°C, respectively.

3. RESULTS AND DISCUSSION

3.1 Copper-glycine chemistry

There is a well-defined aqueous chemistry of Cu^{2+}, and a large number of salts of various anions, many of which are water soluble, exist in addition to a wealth of complexes. The aqua ion $[Cu(H_2O)_6]^{2+}$ is tetragonally distorted both in crystals and in solution [12]. Glycine, H_2NCH_2COOH, is the simplest amino acid, which exists under three different forms in aqueous solutions depending on

the pH value: $^+H_3NCH_2COOH$ (cation), $^+H_3NCH_2COO^-$ (zwitterion), and $H_2NCH_2COO^-$ (anion). These species are denoted as: H_2G^+, HG, and G^-, respectively, for brevity. The equilibria between these may be depicted as [13]:

$$^+H_3NCH_2COOH \underset{(H_2G^+)}{\overset{K_{a1}}{\rightleftharpoons}} {}^+H_3NCH_2COO^- \underset{(HG)}{\overset{K_{a2}}{\rightleftharpoons}} H_2NCH_2COO^- \atop (G^-) \tag{1}$$

which are characterized by the equilibrium constants:

$$K_{a1} = \frac{[HG][H^+]}{[H_2G^+]} \tag{2}$$

$$K_{a2} = \frac{[G^-][H^+]}{[HG]} \tag{3}$$

The pK's values of glycine are: $pKa_1 = 2.07$ and $pKa_2 = 9.97$ at 25°C [13-15].

Depending on the copper concentration, the glycine concentration and pH, glycine molecules can successively replace water molecules in copper's coordination sphere, forming copper-glycine complexes. An important point is to understand the deposition solution chemistry and especially the copper species involved in the deposition process. In aqueous solutions, Cu(II) soluble species are Cu^{2+}, hydroxide complexes, chloride complexes and glycine complexes. The concentration of the latter are related to Cu^{2+} concentration by the equilibrium reaction:

$$Cu^{2+} + iL^- \leftrightarrow CuL_i^{(2-i)} \tag{4}$$

each complex is characterized by its stability constant $\beta_i^{L^-}$.

$$\beta_{iCu}^{L^-} = \frac{\left[CuL_i^{(2-i)}\right]}{[L^-][Cu^{2+}]} \tag{5}$$

where L^- represents a ligand, OH^-, Cl^- or G^-, in the present work, and i the coordination number. The values of $\beta_{iCu}^{L^-}$ were obtained from literature [13-15] and are reported in Table 2.

$$\beta_{iCu}^{L^-} = \frac{\left[CuL_i^{(2-i)}\right]}{[L^-][Cu^{2+}]}$$

In addition, when the pH increases, there is an increasing tendency for the formation of metal hydroxide. With copper cations, this equilibrium can be expressed by the following equilibriums:

$$Cu(OH)_{2(s)} \leftrightarrow Cu^{2+} + 2OH^- \tag{6}$$

characterized by the solubility constant K_s.

$$K_s = [Cu^{2+}][OH^-]^2 \tag{7}$$

Table 2. Equilibrium constants for the overall formation of complexes for the copper-glycine-chloride-water system and the hydroxide solubility product obtained from the literature [13-15]

	L = OH⁻				L = Cl⁻				L = G⁻		pK$_s$
i =	1	2	3	4	1	2	3	4	1	2	
	6.1	13.0	14.7	15.8	0.06	0.73	0.93	0.16	8.1	15.1	19.35

From the values of $\beta_{iCu}^{L^-}$ and K_s, it is possible to construction of species repartition and pH-E diagrams. The species repartition-pH diagrams were computed using the definition of complexation coefficient of Cu(II), $\alpha_{Cu(L=G^-,OH^-,Cl^-)}$ [16]. It is defined as: the ratio $c_{Cu}/[Cu^{2+}]$, where c_{Cu} is the total concentration of copper including all complexes, $[Cu^{2+}]$ and $[Cu(OH)_{2(s)}]$; and $[Cu^{2+}]$ is the concentration of free copper cations Cu^{2+}.

$$\alpha_{Cu(L=G^-,OH^-,Cl^-)} = \frac{c_{Cu}}{[Cu^{2+}]} = \frac{[Cu^{2+}] + \Sigma\left[CuL_i^{(2-i)}\right] + [Cu(OH)_{2(s)}]}{[Cu^{2+}]} \tag{8}$$

Combining Equations (5), (7) and (8), $\alpha_{Cu(L=G^-,OH^-,Cl^-)}$ can be expressed as:

$$\alpha_{Cu(L=G^-,OH^-,Cl^-)} = 1 + \sum \beta_{iCu}^{L^-}[L^-]^i + K_s\frac{(K_w)^2}{[H^+]^2} \tag{9}$$

Using this last equation, one can easily calculate the distribution of different species:

$$\%Cu^{2+} = \frac{100}{\alpha_{Cu(L^-=G,OH,Cl)}} \tag{10}$$

$$\%CuL_i^{(2-i)} = \beta_{iCu}^{L^-}[L^-]\%Cu^{2+} \tag{11}$$

$$\%Cu(OH)_{2(s)} = \%Cu^{2+}\frac{K_s(K_w)^2}{[H^+]^2} \tag{12}$$

As a result, the key point of the calculation is the determination of $[G^-]$. In a first step, we can establish the glycine protonation coefficient α_{G^-}, defined as:

$$\alpha_{G^-} = \frac{[G^-] + [HG] + [H_2G^+]}{[G^-]} = 1 + \frac{[H^+]}{K_{a1}} + \frac{[H^+]^2}{K_{a1}K_{a2}} \tag{13}$$

It must be pointed out that under our experimental conditions α_{G^-} differs from the $c_{G^-}/[G^-]$ ratio, where c_{G^-} is the overall-glycine concentration, assuming that a significant part of glycine ions is involved in the formation of complexes. Then, this ratio can be expressed as:

$$\frac{c_{G^-}}{[G^-]} = \alpha_{G^-} + \frac{[CuG] + 2[CuG_2]}{[G^-]} \tag{14}$$

leading to a second degree equation:

$$2\beta_{2Cu}^{G^-}\frac{c_{Cu}}{\alpha_{Cu(L=G^-,OH^-,Cl^-)}}[G^-]^2 + \left(\alpha_{G^-} + \beta_{1Cu}^{G^-}\frac{c_{Cu}}{\alpha_{Cu(L=G^-,OH^-,Cl^-)}}\right)[G^-] - c_{G^-} = 0 \tag{15}$$

The determination of $[G^-]$ can be achieved by an iterative method involving Equations (13), (14) and (15). Then, using equations (10-12) one can easily obtain the distribution diagram for the copper-glycine-chloride-water system. The Figure 1 shows the species repartition diagram obtained.
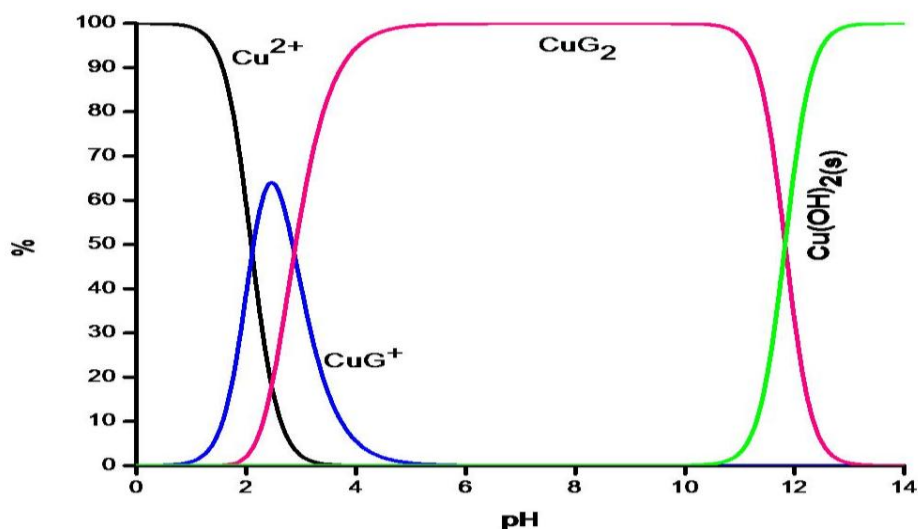

Figure 1. Species distribution diagram as a function of the solution pH for the copper-glycine-water system at 25°C. This diagram was constructed under these conditions: 0.1 M Cu(II) + 0.2 M Cl⁻ + 1.2 M Glycine.

Figure 1 shows the species repartition diagram obtained from Relations (11-13) and considering the conditions displayed in Table 1 for solution S_0. In this diagram it is possible to observe four characteristic pH regions. The first region is characterized by the free copper ions as the most stable species (pH region 0-2). In the second region, between pH 2 and pH 4, the predominant copper species are CuG^+. In the third region, from pH 3 to pH 12, the predominant copper species are CuG_2 complexes. The fourth region, above pH 12, is characterized by one copper hydroxides; the predominant copper hydroxide is the insoluble species $Cu(OH)_{2(s)}$.

These results clearly indicate that under our experimental conditions the neutral 1:2 CuG_2 complexes predominates in the solutions S_1 and S_2 mentioned in Table 1.

Based on the information provided by the species repartition diagrams, we have constructed the E-pH diagram for values of pH above 4. Figure 2 shows the E-pH diagram for the copper-glycine-chloride-water system at 25°C. In this work, the conditions listed in Table 2 for solution S_1 are used in constructing Pourbaix diagram. The most stable forms of copper soluble/insoluble species are indicated in the diagram and have seen determined from the solution chemistry. The Pourbaix diagram developed shows the dependence of the equilibrium potential for the redox couple Cu(II)/Cu(0) on the glycine concentration at different pH values.
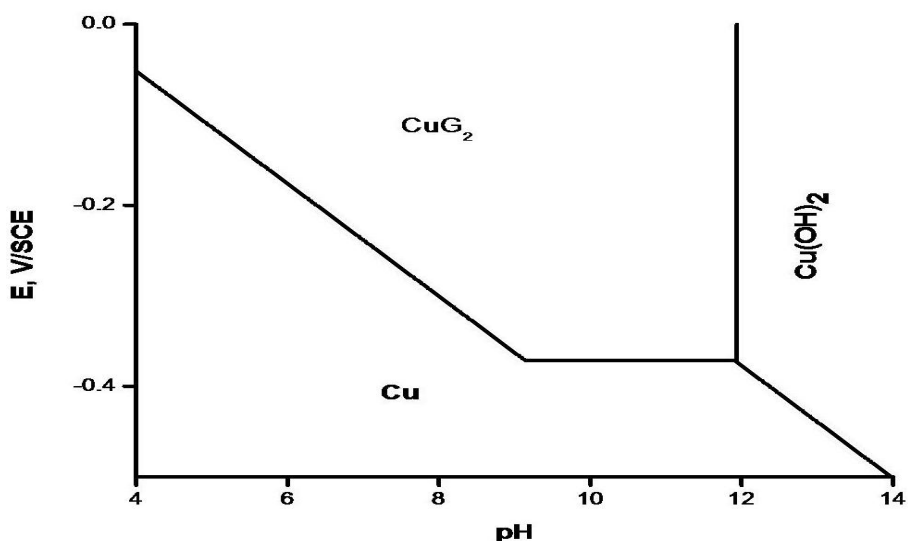

Figure 2. Potential-pH diagram for the reduction of Cu(II)' species. The set conditions considered in the computation of this diagram are also same that in Figure 1.

Figure 2 is an enlarged view of the diagram in the copper deposition region. For pH values between 4 and 9, the Figure 2 indicates that increasing pH displaces the equilibrium potentials toward more negative values. For pH values between 9 and 12 the equilibrium potential is keep constant value. On the basis of these results, we therefore assume that under our experimental conditions the overall reaction of copper electrodeposition process at pH 10.0 will be the following:

$$CuG_2 + 2e^- \overset{\vec{k}}{\to} Cu^0 + 2G^- \qquad (16)$$

The conditional (formal) potential of the reaction (16) at 25°C is given by:

$$E_{eq}^{0'}(CuG_2/Cu(0)) = -0.347 - 0.0592 \log[G'] + 0.0296 \log[Cu(II)'] \qquad (17)$$

where:

$E_{eq}^{0'}(CuG_2/Cu(0))$ represents the equilibrium potential, in Volts *vs.* SCE, for the redox couple $CuG_2/Cu(0)$. The generalized notation Cu(II)' represents the free copper ions in the solution, the

soluble copper-glycine complexes, or the metal hydroxide in either soluble or insoluble form; G'
corresponds with the free concentration of glycine: $[G'] = [H_2G^+] + [HG] + [G^-]$..., etc.

The Eq. (17) allows one to predict a displacement in the value of equilibrium potential when
there is a change glycine and/or copper ions concentration at 25°C. In sum, is important to mention
that the overall reaction Eq. (16) of the chemical species CuG_2 is the same as proposed Kublanovsky-
Litovchenko [9] in alkaline medium using chronopotentiometric measurements in the Cu(II)-glycine
system.

3.2. Voltammetric study

Cyclic voltammetry study was performed in the potential range 0 to -1.0 V *vs.* SCE on nickel
electrode from solutions S_0, S_1 and S_2. The potential scan was initiated in the negative direction from
the open circuit potential (E_{OCP}) at different scan rates (υ) between 10-500 mV s^{-1}.
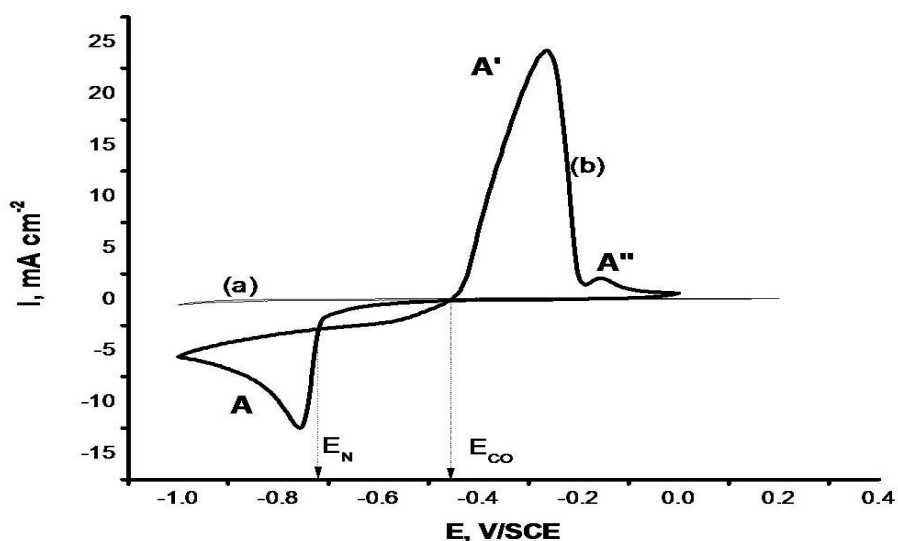

Figure 3. Typical cyclic voltammograms obtained onto nickel electrode from electrolytic solutions: (a)
S_0 and (b) S_1 at pH 10 and 25°C. Scanning rate: 10 mV s^{-1}.

Typical cyclic voltammograms obtained from solutions S_0 and S_1 are presented in Figure 3 at
10 mV s^{-1}. The cyclic voltammogram corresponding to curve (a) in Figure 3 shows that in absence of
copper ions in solution there was no current produced. The curve (b) in Figure 3 shows the cyclic
voltammogram obtained from solution S_1; this voltammogram presents the following characteristics: a
negligible cathodic current was observed from the E_{OCP} to -0.6 V *vs.* SCE indicated no reaction in this
potential range; continuing with the potential scan in the negative direction is possible to observe the
formation of one cathodic peak, A, at the peak potential -0.758 V *vs.* SCE. We associate this peak with
the reduction of the chemical species CuG_2 to Cu(0), as was proposed in Eq. (16).

When the scan direction was reversed in the switching potential E_λ = -1.0 V *vs.* SCE, two
crossovers (E_{CO} and E_N) between the current density anodic and cathodic are observed, a feature that is

characteristic of the formation of a new phase [17, 18]. The E_N potential is just a crossover potential at which nucleation and growth take place with a measurable rate. The E_{CO} potential is known as the crossover potential and this is associated with $E_{eq}^{0'}(CuG_2/Cu(0))$. Is important to mentioned that the value of E_{CO} (-0.456 V *vs.* SCE) is approximately the predicted value from Eq. (17). The $E_{eq}^{0'}(CuG_2/Cu(0))$ value obtained from of Eq. (16) is -0.377 V *vs.* SCE. Difference of 79 mV, between E_{CO} and $E_{eq}^{0'}(CuG_2/Cu(0))$ was found for S_1. This difference might be associated to adsorption process or formation of chemical species in the interphase. Under the above conditions, we propose that there is a good approximation between E_{CO} and $E_{eq}^{0'}(CuL_2^{2-}/Cu(0))$, and that Eq. (16) represents the copper electrodeposition. At potentials more positive than E_{CO}, two anodic peaks, A' and A'', are observed; these peaks could be associated with the oxidation of the previously Cu deposited in peak A. The difference between the $E_{eq}^{0'}(CuL_2/Cu(0))$ value and potential value (E_N) at the onset of growth of copper crystals is known as the nucleation overpotential [19]. The difference between the E_N and E_{CO} values can be employed to estimate the experimental value of nucleation overpotential [20]. The value of the nucleation overpotential obtained is 265 mV.

In our experiments, the difference between the anodic A' and cathodic A peak potentials ($\Delta E_P = E_{PA} - E_{PA'}$), for cyclic voltammogram in Figure 3, is 0.497 V for solution S_1. The obtained value for ΔE_P significantly exceed the quantity characteristic of a reversible process, $\Delta E_P = 0.059/n$ at 25°C and n = 2 [17, 21]. Therefore, we could assume that a totally irreversible reaction might be the case, from the cyclic voltammograms recorded (Figure 3). From curve (a) in Figure 3 one can determine the magnitude of the product $\alpha_c n_\alpha$, where α_c is the cathodic transfer coefficient and n_α is the number of electrons transferred up to, and including, the rate determining steps. With this purpose, such a parameter of the mentioned cyclic voltammograms as the shape factor $\left|E_{PB} - E_{PB/2}\right|$ can be applied [17, 21]:

$$\left|E_{PB} - E_{PB/2}\right| = \frac{48}{\alpha_c n_\alpha} \text{ mV at 25°C} \tag{18}$$

where $E_{PB/2}$ is the potential of a half-peak. It was found that $\alpha_c n_\alpha \approx 1.71$, if the reaction (16) is considered as totally irreversible.

3.2 Effect of the potential scan rate

The effect of scanning rate on cyclic voltammograms from solution S_1 is given in Figure 4. The voltammograms, all initiated from the E_{OCP}, were scanned in the negative direction at rates ranging from 50 to 500 mV s^{-1}.
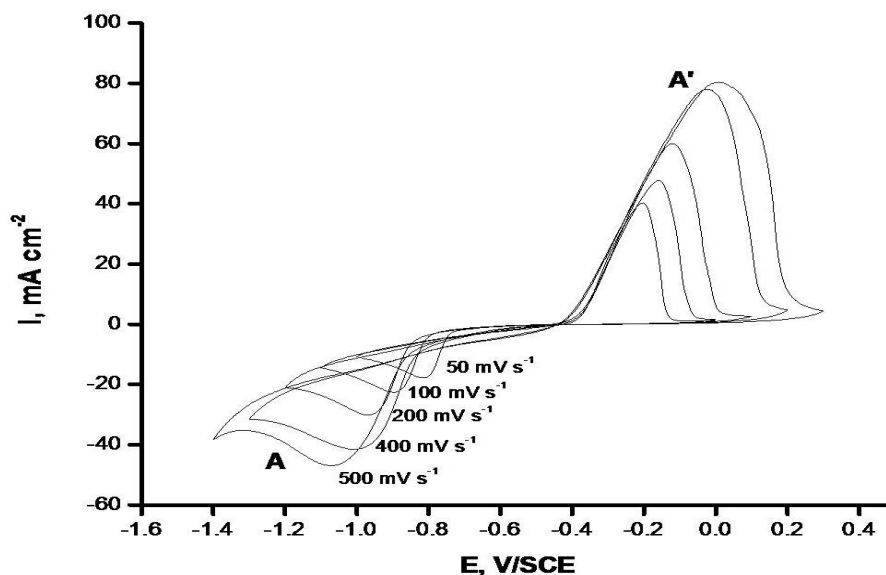
Figure 4. Cyclic voltammograms obtained onto nickel electrode at different scan rates from solution S_1 at 25°C.

According to Figure 4, all voltammograms are characterized by one cathodic (A) and anodic (A') peak. The cathodic peak maximum currents (i_c) were found to increase and the cathodic peak potentials (E_p) shifted negatively when υ was increased during the scan.

In either case, the maximum current value of the peak A was found to be proportional to the square root of the sweep rate within the range of sweep rates applied (Figure 5(a)), indicating a diffusion-controlled process [17, 21].

The cathodic peak potentials E_P shift in the negative direction, as mentioned above, and are nearly linear with respect to the decimal logarithm of the sweep rate (Figure 5b), suggesting that the reaction (16) is not reversible and tentatively may be considered as irreversible. Then, from the variation of E_P with log υ given by the following equation [17, 21]:

$$E_p = K - (2.3RT/2\alpha_c nF) \log \upsilon \tag{19}$$

where

$$K = E° - (RT/\alpha_c n_\alpha F)[-0.78 - (2.3/2)\log(\alpha_c n_\alpha FD/k_s^2 RT)] \tag{20}$$

K_s is the standard rate constant, and the other terms have their usual significance, it should be expected that E_P shifts by $30/\alpha_c n_\alpha$ mV for each decade increase in υ. However, as is evident from curve (b) in Figure 5, the experimental shift of E_P for the solution S_1 with increasing υ from 10 to 100 mV s^{-1} is equal to 136 mV. Quite apparently, such values of the negative shift of E_P for each decade increase in υ are in a considerable excess of that expected for the totally irreversible reaction [17, 21]. These features of cyclic voltammograms recorded in this work clearly show that the diagnostic criteria for a

totally irreversible system reported in the literature [17, 21] are not wholly satisfied. Consequently, the reaction (16) could not be considered as a simple irreversible reaction.
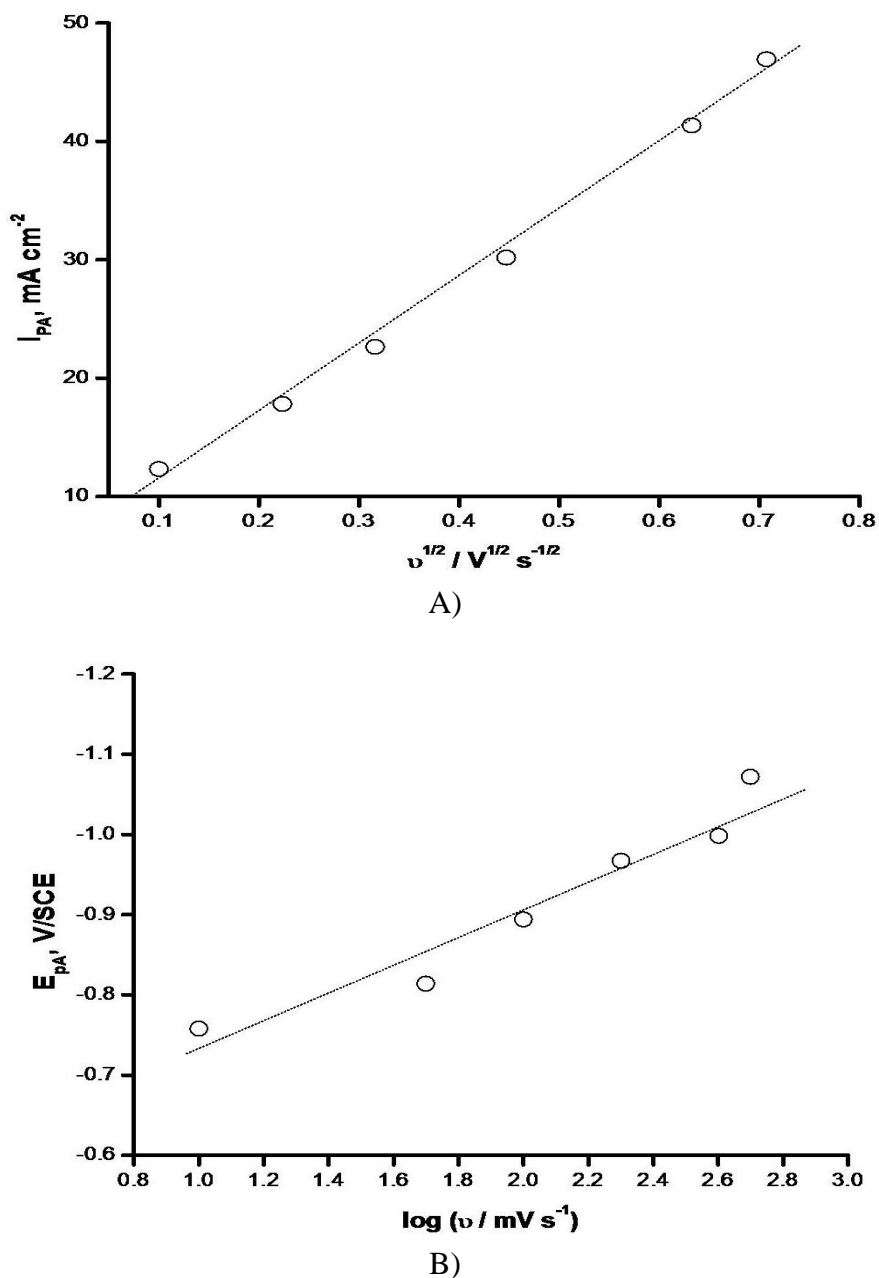

A)

B)

Figure 5. Variation of current density maxima i_P and potential E_P for peak A in cyclic voltammograms as a function of the scan rate. (a) i_{PA} vs. $\upsilon^{1/2}$ and (b) E_{PA} vs. log υ.

3.2.2 Effect of glycine concentration

Effect of glycine concentration on the copper reduction mechanisms was studied from solution S_2. The results are presented in Figure 6, where curves (a) and (b) are represented by dotted and solid lines, respectively. The voltammograms (a) and (b) were obtained from solutions S_1 and S_2, respectively, at 10 mV s^{-1} and 25°C.
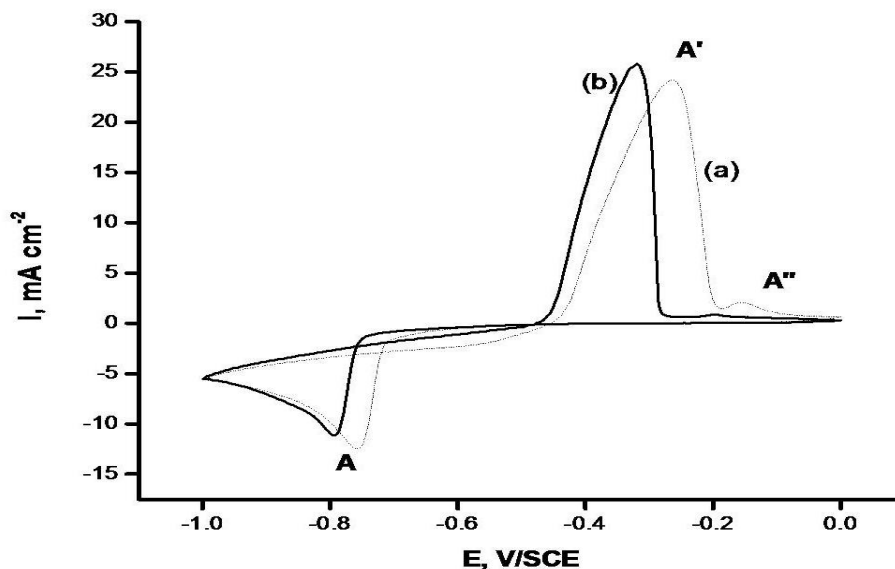
Figure 6. Typical cyclic voltammograms obtained on nickel electrode from solutions: (a) S_1 and (b) S_2 at 25°C. Scanning rate: 10 mV s^{-1}.

In the Figure 6 is possible to observe that when glycine concentration is increased some effects on the response in the voltammogram are found. A comparison of voltammograms obtained from of the solution S_1 (curve a, Fig. 6) and S_2 (curve b, Fig. 6) allows the study of this effect. In Figure 6 can be to observed that the peak potential (E_{PA}) and the cathodic peak current density intensity (i_{PA}) are depending of the composition of the solution. During the forward scan towards negative potentials, a fast increase in the cathodic current is observed, giving rise to peak A, associated with the electrodeposition of copper. Evidently when the glycine concentration increases, the peak A is more negative.

This displacement of copper reduction potential to more negative values, known as cathodic polarization, has been reported in the literature [19] for other metals in presence of organic compounds. In sum, the cathodic current of peak A is diminished with an increase of glycine concentration and there is also a change in the E_{CO} and E_n values is observed, see Table 3. The value of the nucleation overpotential obtained is 273 mV for solution S_2, which is similar than that obtained from solution S_1. These results indicate that the electrocrystallization process, from solutions S_1 and S_2, requires similar energy to obtain thermodynamically stable nuclei and start the growth of copper onto the nickel electrode surface.

The cathodic charges (Q_C) associated with the peak A were obtained by integration from the voltammetric curves and are shown in Table 3.

These results indicate that the increasing of glycine concentration in solution, the quantity of copper deposited in this potential range decreases by 21% with respect to that deposited from solution S_1. Also the anodic charges (Q_A) associated with the peak A' were obtained. Table 3 lists the values of Q_A/Q_C for each solution. We highlight that the value of Q_A/Q_C ratio does not depend on the glycine concentration in the electrolytic solution.

3.2.3 Effect of temperature

The effect of temperature on cyclic voltammetry was studied from solution S_1 and this is shown in Figure 7. The voltammograms were obtained at 25°C and 40°C and these are represented by dotted and solid lines, respectively. The only effects found were the increase of current density and a displacement of copper reduction potential to more positive values with an increase of temperature.
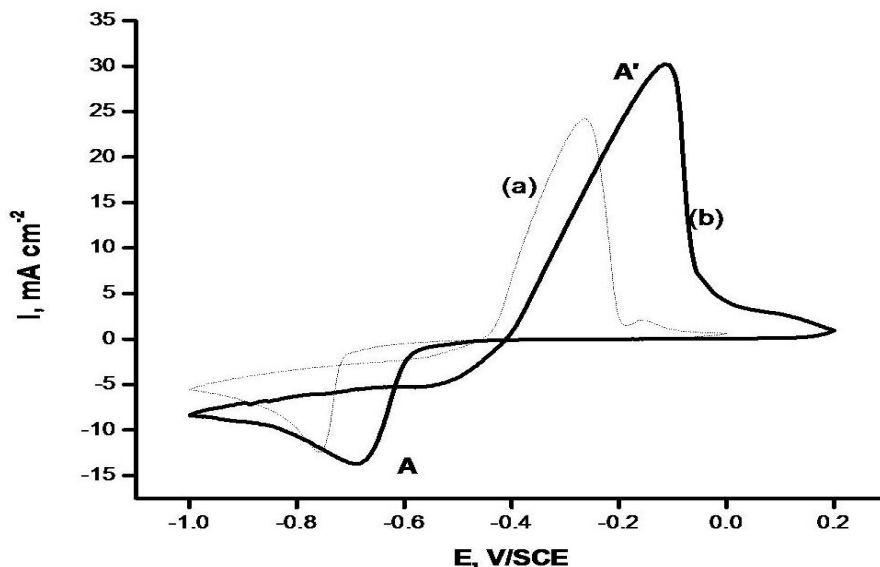

Figure 7. Figure 6. Typical cyclic voltammograms obtained on nickel electrode from solution S_1 at different temperatures: (a) 25°C and (b) 40°C. Scanning rate: 10 mV s^{-1}.

Table 3. Values of thermodynamic parameters characteristics obtained from voltammetric study.

Solution	$E_{eq}^{0'}$	E_N	E_{CO}	E_{PA}	$E_{PA'}$	Q_C/Q_A
	V/SCE	V/SCE	V/SCE	V/SCE	V/SCE	-
$S_{1\ (25°C)}$	-0.377	-0.721	-0.456	-0.758	-0.261	0.93
$S_{1\ (40°C)}$	–	-0.615	-0.410	-0.688	-0.117	0.92
$S_{2\ (25°C)}$	-0.394	-0.757	-0.484	-0.790	-0.264	0.91

In sum, there is also a change in the E_{CO} and E_n values is observed, see Table 3. The value of the nucleation overpotential obtained is 205 mV for solution S_1 at 40°C, which is smaller than that obtained from solution S_1 at 25°C. These results indicate that the electrocrystallization process, from solutions S_1 at 40°C, requires a smaller energy to obtain thermodynamically stable nuclei and start the growth of copper onto the nickel electrode surface.

The cathodic charges (Q_C) associated with the peak A were obtained by integration from the voltammetric curves and are shown in Table 3. As shown in Table 3, these results indicate that the increasing of the temperature of the solution causes an 86 % raise in the reduction of copper. Also the anodic charges (Q_A) associated with the peak A was obtained. Table 3 lists the values of Q_A/Q_C for each solution. We highlight that the value of Q_A/Q_C ratio does not depend on the temperature of the electrolytic solution.

3.3. Voltammetric study in the stationary diffusion regime

The electrochemical reduction of copper in the stationary diffusion regime was studied using the rotating disk electrode (RDE) voltammetry technique. For a given temperature, a constant potential scan rate (1 mV s^{-1}) was imposed and the electrode rotation rate (Ω) was varied from 100 to 2500 rpm. Before each run, a Cu predeposit was prepared in situ on glassy carbon electrode of 0.20 cm^2 visible surface area by applying 20 mA cm^{-2} for 20 s.
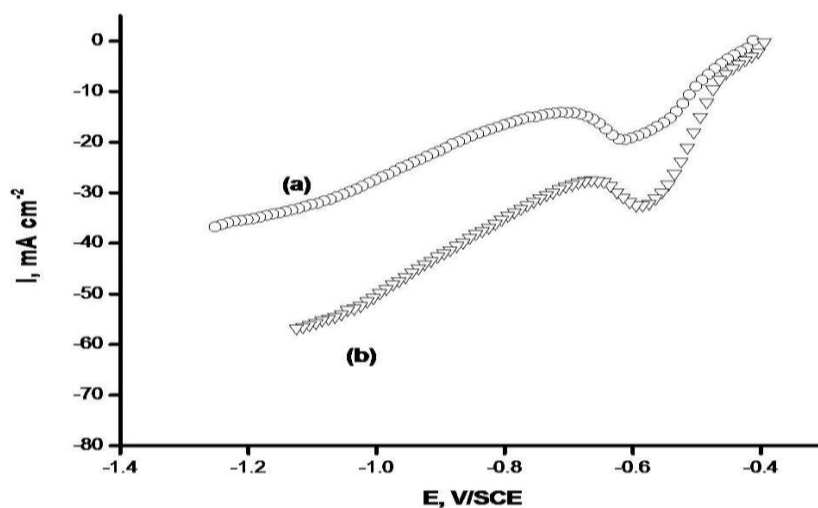

Figure 8. Typical linear voltammograms recorded using a RDE, obtained during the electroreduction of copper from solution S$_1$ at different temperatures: (a) 25ºC and (b) 40ªC

Figure 8 shows a comparison between two experimental curves of i *vs.* E obtained from the electrolytic solution at 25°C (curve a, Figure 8) and 40ºC (curve b, Figure 8), respectively. For each of the temperatures, the classical limiting current density (i$_L$) exhibited a linear variation with $\Omega^{1/2}$, as can be seen in Figure 9. This behavior demonstrates that, for both temperatures, the reduction of Cu(II) ions is limited by mass transfer of the electroactive species. Extrapolating the curves i$_L$ *vs.* $\Omega^{1/2}$ to $\Omega^{1/2}$ = 0 yields a nonzero current density for each temperature, indicating that the current density is additionally enhanced by other phenomena coupled to the charger transfer process.

Voltammograms in Figure 8 contain pre-waves and even maxima; similarly behavior has been reported by Survila et al. [7] at 20ºC. To explain this behavior, Survila et al. [7] have proposed that the

copper reduction process at alkaline pH, it occurs on the surface covered by Cu_2O if the first rise of the voltammograms is under discussion.

To analyze the effects of temperature on the Cu cathodic process, we have chosen the global mechanism given by Eq. (16).
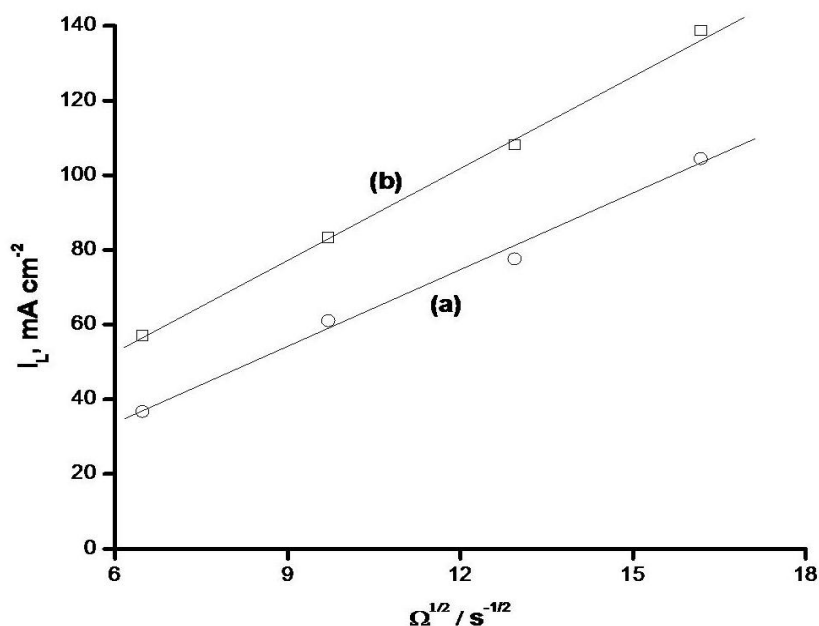

Figure 9. Variation in the cathodic limiting current density with agitation, obtained from solution S_1 at different temperatures: (a) 25°C and (b) 40°C.

3.3.1 Calculation of diffusion coefficients

The values of the diffusion coefficient (D) for the CuG_2 species were calculated using the well-known Levich equation Eq. (21) [17, 21]. It gives a relationship between the diffusion-convection limiting current density, i_L, obtained on a rotating disk electrode (RDE), the electroactive species concentration, c, diffusion coefficient, D, the solution kinematic viscosity, ν, and the revolution rate of the RDE, Ω.

$$i_L = 0.620nFD^{2/3}\nu^{-1/6}c\Omega^{1/2} \tag{21}$$

From the slopes of the lines shown in Figure 9, the values of diffusion coefficients of CuG_2 were calculated at different temperatures using Eq. (21) and the values obtained are: $D_{25°C} = 3.8 \pm 0.2$ x 10^{-6} cm^2 s^{-1} and $D_{40°C} = 6.6 \pm 0.1$ x 10^{-6} cm^2 s^{-1}.

From these calculations is possible to know the value of the radius of CuG_2 complexes; the ratio $D\eta/T$ was calculated, where η is the dynamic viscosity in poise. The value obtained shows that the product $D\eta/T$ is satisfactorily constant and independent from temperature and viscosity of the

solutions. Its average value is $(1.66 \pm 0.07) \times 10^{-10}$ cm^2 poise/s K. The constancy of the term Dη/T can be interpreted according to the Einstein-Stokes theory,

$$\frac{D\eta}{T} = \frac{k}{6\pi r} \tag{22}$$

In Eq. 22 r is the average radius of the diffusion entity. From the average value of Dη/T and taking $k = 1.38 \times 10^{-23}$ J/K, Eq. 22 yields $r = (4.40 \pm 0.02) \times 10^{-8}$ cm, which is an acceptable figure for the average apparent radius of copper complexes. Similar values have been reported in the literature for Cu(II) complexes with ligands used in alkaline solutions [22, 23].

3.3.2 Calculation of kinetic parameters

We determined the kinetic parameters from the current density/potential data corresponding to the second increase.

In the case of an irreversible electrode process, the current any potential in the region of mixed control is given by the kinetic equation [17, 21]:

$$\frac{1}{i} = \frac{1}{nF\vec{k}C} + \frac{1.61v^{1/6}}{nFCD^{2/3}} \frac{1}{\Omega^{1/2}} \tag{23}$$

in Eq. (23) $\vec{k}$ (cm s^{-1}) is the rate constant for cathodic process, which is defined by:

$$\vec{k} = \vec{k}_o \exp\left[-\frac{\alpha_c nF\left(E - E_{eq}^{o\prime}\right)}{RT}\right] \tag{24}$$

Here, $\vec{k}_o$ (cm s^{-1}) is the rate constant for cathodic process at $E_{eq}^{o\prime}$ V vs. SCE, α_c is the charge transfer coefficient for cathodic reaction.

The kinetic parameter $\vec{k}_o$ was evaluated by plotting i^{-1} vs. $\Omega^{-1/2}$ for several constants potentials in the intermediate zone and then to extrapolate the current density to $\Omega = \infty$. Figure 10 shows typical i^{-1} vs. $\Omega^{-1/2}$ curves obtained from voltammograms shown in Figure 8 at several potentials. It can be seen that the plot i^{-1} vs. $\Omega^{-1/2}$ is linear, and the intercept can be used to calculate $\vec{k}_o$. Moreover, the slopes $\left(\frac{d|i^{-1}|}{d\Omega^{-1/2}}\right)$ of these plots are independent of potential, while the intercepts vary strongly with potential for each temperature.

Using the values of $\vec{k}_o$ obtained for each potential, it was possible to estimate the kinetic parameters $(\vec{k}_o \text{ and } \alpha_c)$ from the Eq. (24).

The value of $\vec{k}_o$ increases from $(2.2 \pm 0.3) \times 10^{-6}$ m s^{-1} to $(5.9 \pm 0.1) \times 10^{-6}$ m s^{-1} when the temperature was increased. These findings indicate that the reduction kinetics is slower at 25°C, as expected. In addition, the values of the charge transfer coefficient ($\alpha_c \approx 0.1$) obtained are independent of the temperature. It is important to note that the values $\vec{k}_o$ obtained in the present study are similar to the obtained by Survila et al. [7]
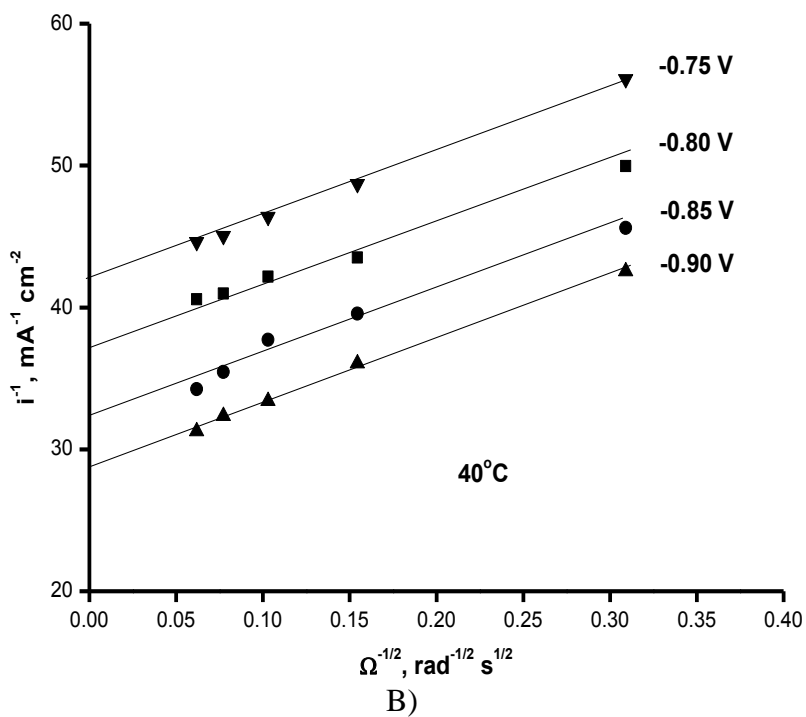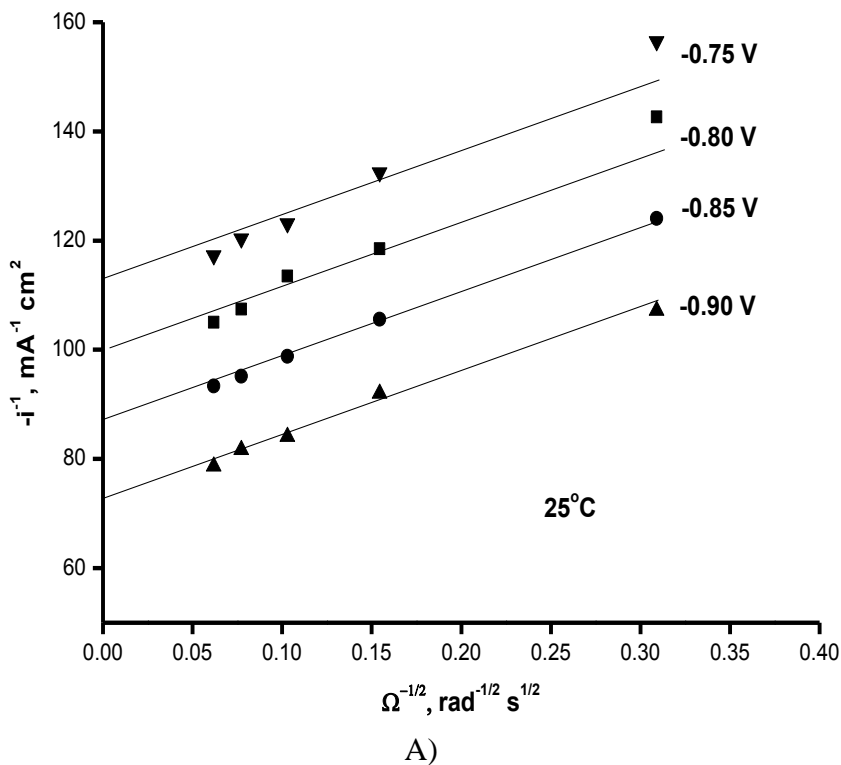
Figure 10. i^{-1} versus $\Omega^{-1/2}$ plots a function of potential a different temperatures: (a) 25°C and (b) 40°C.

3.4. Characterization of the copper coatings

The copper coatings on nickel substrates obtained from electrolytic solution at 25°C and 40°C were analyzed using SEM and XRD. The deposits were grown potentiostatically at same potential value, E = -0.8 V vs. SCE, during three minutes for both temperatures.

The morphological features (Figure 11) at 25°C and 40°C of copper coatings are now presented and correlated to the results discussed before. Figure 11(a) shows that irregular and coarse coatings are produced in the solution S_1 at 25°C. By X-ray diffraction analysis (Figure 12), was confirmed the only presence of copper and nickel in the coating obtained in solution S_1 at 25°C. In contrast to the morphology of the copper coating formed at 25ºC, the Figure 11(b) shows that the copper coatings obtained at 40°C are less refined coatings and also irregular and coarse. These coatings were produced with reaction rate bigger and presented a decreasing in the overpotential for the discharge of copper ions, as already seen in Figure 7. Figure 12 shows that coatings are formed of copper pure. It is important to note that golden electrodeposits were successfully obtained at 25ºC and 40ºC.
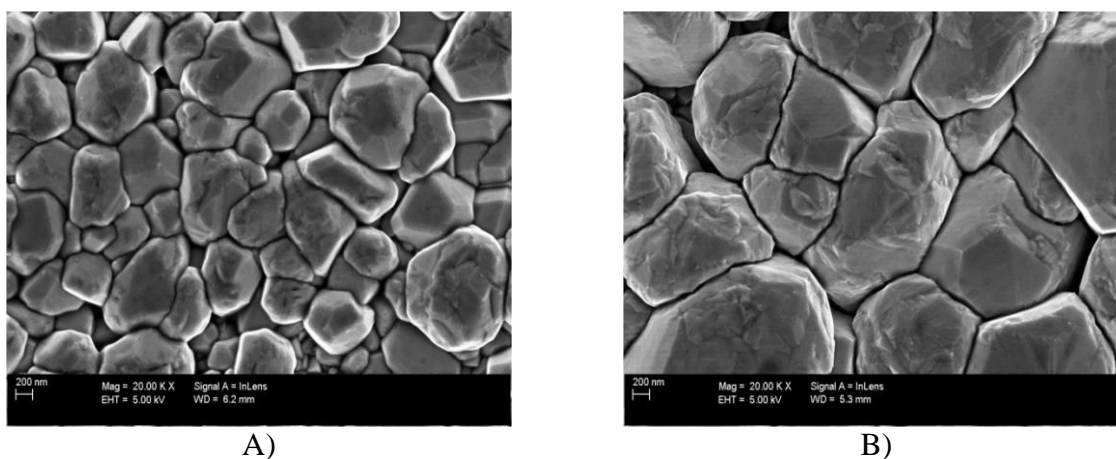

A)   B)

Figure 11. SEM images of deposits previously formed during 3 minutes in the electrolytic solution at different temperature: (a) 25ºC and (b) 40ºC.

At 25ºC the copper coating forms a complete uniform layer of fine-grain less than 1.2 μm size (Figure 11a). In contrast to the morphology of the copper coating formed at 25ºC, the copper deposit obtained at 40ºC onto nickel electrode resulted in a layer of less than 2.2 μm grain size (Figure 11b). In general, is important to mention that the average grain size at 25ºC is smaller than at 40ºC, which is the effect of temperature on the acceleration of the electrochemical reaction kinetic.

The deposit crystallographic structures were characterized by XRD (Figure 12). We have quantified the variation of the crystallite size ($D_{Cu(hkl)}$) with the deposition temperature, it has been determined here from the full width at half maximum (fwhm) of the Cu lines by means of the Scherrer's formula:

$$D_{(hkl)} = \frac{0.89\lambda}{b \cos\theta} \tag{25}$$

where λ is the wavelength of the incident beam, b the corrected fwhm of the line (rad)(2θ) and θ is the diffraction angle. The results have been only calculated for the diffraction peak indexed by the Cu(111) reflection. At 40ºC, $D_{Cu(111)}$ is larger than $D_{Cu(111)}$ obtained a 25ºC.
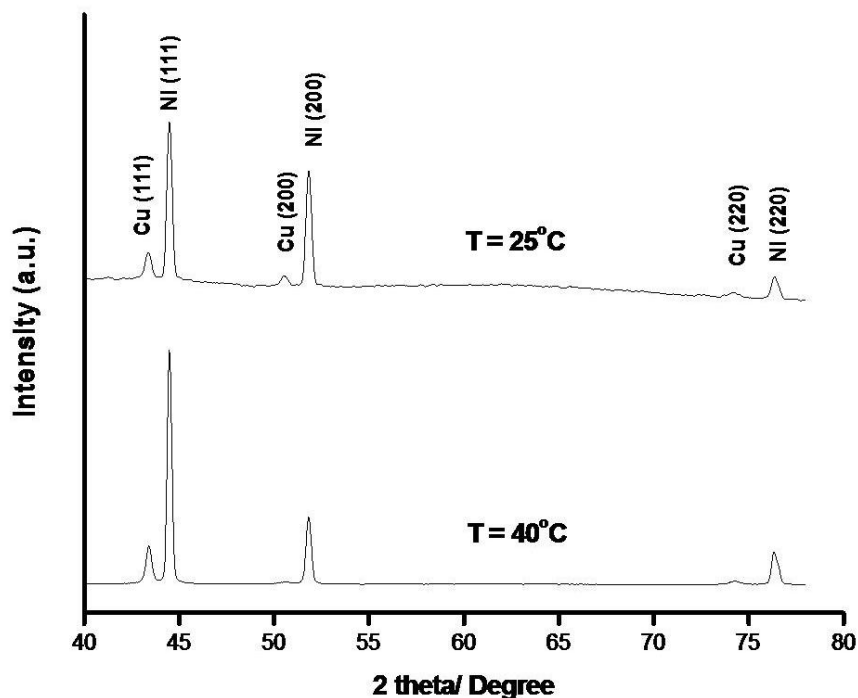
Figure 12. Effect of deposition temperature on the X-ray diffraction patterns. The scale can vary from one sample to another.

4. CONCLUSIONS

Copper coatings can be produced from non-cyanide alkaline solutions containing glycine. The use of glycine as a ligand produces stable copper complexes and homegeneous coatings. This organic compound seems to act not only as a leveling agent, but also as a new and efficient ligand, since it directly increases the quality of the coatings.

The thermodynamic study has lead to the conclusion that the predominant chemical species of copper in the electrolytic solution are CuG_2 and the overall reaction involved in the copper electrodeposition process is proposed.

Changes in the thermodynamic parameters, morphology and parameters kinetics during the electrocristallization of copper are observed when the temperature in changed. The effect of the temperature is reflected on the nucleation potential (E_N) value. Highest E_N value was obtained at 25ºC, these result showed that at 40ºC requires the smaller energy to obtain the bulk deposition. Thus, was found that the increasing of temperature in solution causes an 86% raise in the reduction of copper.

From voltammetric study in the stationary diffusion regime, it was possible to evaluate the charge transfer coefficient (α_c) and rate constants ($\vec{k}$) of global copper reduction process. The values obtained shown that the rate of reduction reaction of copper is faster at 40ºC.

Micrographs SEM images of the deposits obtained on nickel substrate at different temperature shown that the average grain size is smaller at 25ºC. However, the morphology of both coatings (at

25°C and 40ºC) shown a range of grain sizes. It is important to note that golden electrodeposits were successfully obtained at 25ºC and 40ºC.

References

1. M. Schlesinger, M. Paunovic, *Modern Electroplating*, John Wiley & Sons, Inc., New York (2000)
2. I.Rodriguez-Torres, G. Valentin, S. Chanel and F. Lapicque, *Electrochim. Acta,* 46 (2000) 279
3. A.E. Mohamed, S. M. Rashwan, S. M. Abdel-Wahaab, M. M. Kamel, *J. Appl. Electrochem*., 33 (2003) 1085
4. S. M. Rashwan, A. E. Mohamed, S. M. Abdel-Wahaab and M. M. Kamel, *J. Appl. Electrochem.,* 33 (2003) 1035
5. J. L. Ortiz-Aparicio, Y. Meas, G. Trejo, R. Ortega, T. W. Chapman, E. Chainet and P. Ozil, *Electrochim. Acta*, 52 (2007) 4742
6. A.Survila and V. Uksiene, *Elektrokhimiya*, 25 (1989) 952
7. A.Survila and V. Uksiene, *Electrochim. Acta*, 37 (1992) 745
8. A.Survila, P. Kalinauskas and V. Uksiene, *Electrochim. Acta*, 38 (1993) 2733
9. V. Kublanovsky and K. Litovchenko, *J. Electroanal. Chem.,* 495 (2000) 10
10. R. Drissi-Daoudi, A. Irhzo and A. Darchen, *J. Appl. Electrochem.*, 33 (2003) 339
11. J. Uljanionok and A. Survila, *Chemija*, 19 (2008) 20
12. A.Cotton and G. Wilkinson, *Advanced Inorganic Chemistry*, Wiley, New York (1972)
13. R. M. Smith and A. E. Martell, *Critical Stability Constants*, Plenum Press, New York (1989)
14. D. D. Perrin, *Stability Constants of metal-ion complexes*, Pergamon, Oxford (1979)
15. E. P. Serjeant and B. Dempsey, *Ionization Constants of Organic Acids in Aqueous Solution*. Pergamon, Oxford, (1972)
16. B. Tremillon, *Electrochimie Analytique et Reactions en Solution,* Masson, Paris (1993)
17. Southampton Electrochemistry Group, *Instrumental Methods in Electrochemistry*, Ellis Horwood Ltd, Chichester (1985)
18. A.J. Bard and L. R. Faulkner, *Electrochemical methods: fundamentals and applications*, John Wiley & Sons, Inc., New York (2000)
19. G. Gunawardena, G. Hills and I. Montenegro, *J. Electroanal. Chem.,* 184 (1985) 357
20. E. Gileadi, *Electrode Kinetics for Chemists, Chemical Engineers and Materials Scientists*, VCH Publishers, New York (1993)
21. M. Palomar-Pardavé, I. González, A. B. Soto and E. M. Arce, *J. Electroanal. Chem.*, 443 (1998) 125
22. E. Norkus, *J. Appl. Electrochem.,* 30 (2000) 1163
23. A.J. Arvia, J. C. Bazan and J. S. W. Carrozza, *Electrochim. Acta*, 11 (1966) 881